Nucleation and growth of $CaCO_3$ minerals on biomimetic templates studied by small-angle scattering

D. Schwahn,* M. Balz, M. Bartz, A. Fomenko and W. Tremel

Institute for Solid State Research, Research Center Jülich GmbH, D52425 Jülich, Germany, and [b]Institute for Inorganic Chemistry, Johannes Gutenberg-University Mainz, D55099 Mainz, Germany. E-mail: d.schwahn@fz-juelich.de

The process of mineralization of $CaCO_3$ on surfaces built up with DMAP (4-dimethylamino-pyridine) molecules was explored by time resolved SANS experiments. In most samples the DMAP molecules were attached to colloidal gold representing a model system of biomimetic template structures. The small-angle neutron scattering (SANS) data, however, show that DMAP forms in water a more complex structure built up of large (>1000 Å) and small aggregates of about 20 Å radius. The process of $CaCO_3$ mineralization in a 0.1 M aqueous solution of $CaCl_2$ was initiated by thermal decomposition of solid $(NH_4)_2CO_3$ in a closed vessel. This process was followed in-situ by SANS over a time period of about 12 h. Experiments were performed with colloids plus DMAP concentrations between 0 and 49 mg/cm^3 and at two temperatures. A further set of experiments was performed in solution containing a DMAP concentration of 15 mg/cm^3 without colloidal gold. The process of mineralization could be characterized by the time evolution of size and number density of the mineralized particles as will be presented and discussed in this paper.

Keywords: time-resolved neutron diffraction, biomineralization, $CaCO_3$

1. Introduction

The mineralization process of inorganic materials in the presence of organic template structures in nature is still poorly understood and a challenge for scientific research (Mann, 2000). Scattering techniques such as small angle scattering with X-rays and neutrons may have a chance to make important contributions to this problem as they especially allow the exploration of the early stages of mineralization. Especially, small angle neutron scattering (SANS) allows in many cases the characterization of complex structures by applying contrast variation technique and thereby the identification of their different parts as fi. the conformation of polymers or chains in $CaCO_3$ minerals (Endo *et al.*, 2003). In the present case of an aqueous solution contrast variation can be easily applied by using D_2O/H_2O mixtures of different composition and thereby changing the coherent scattering length of the solvent.

In this paper we will present first results of this very new subject. We studied the mineralization of $CaCO_3$ in "pure" water and in the presence of a template structure formed by 4-dimethylamino-pyridine (DMAP) which in most cases was attached to the surface of colloidal gold. Our studies so far were mainly performed in H_2O in order to have good contrast conditions with respect to $CaCO_3$. Although DMAP is not a realistic model of biological template molecules, it allows to obtain aqueous solutions of template covered colloidal gold in a sufficiently high concentration (Gittins & Caruso, 2001) to allow a detailed understanding of the interfacial mineralization processes, which can be useful in an analysis of more realistic models and biological systems.

2. Mineralization of $CaCO_3$ studied by SANS

The process of mineralization was initiated and performed in a special stainless steel container with two sapphire windows for the neutrons and which allows a temperature control from 253 to 373 K (- 20 to 100°C). This cell was mounted in the neutron beam allowing in-situ SANS experiments. The experiments usually took about 12 h and were usually performed at two fixed settings of detector-sample distances of 20 m and 4 m with accumulation times of 15 and 30 min for the first 15 and the following measurements, respectively. The so obtained spectra were analyzed in standard procedure by background subtraction of scattering from pure solvent and by absolute calibration with the secondary standard Lupolen. Changes of the transmission were measured for all spectra and could therefore be considered properly.

The process of mineralization of $CaCO_3$ was performed in a cuvette of optical glass containing a 0.1 M aqueous $CaCl_2$ solution. A CO_2 rich atmosphere was produced by thermal decomposition of $(NH_4)_2CO_3$ at ambient temperature. By combining the decomposition reaction of NH_4CO_3 and the reaction between CO_2 and $CaCl_2$ one obtains the $CaCO_3$ mineral according to

$$(NH_4)_2CO_3 + CaCl_2 \rightarrow CaCO_3 + 2(NH_4)Cl \qquad (1)$$

This gas diffusion technique has the advantage of a sufficiently slow mineralization rate to be detected on the SANS time scale; furthermore, it leads to the same product distribution and morphology as the direct mixing of Ca^{2+} and CO_3^{2-} ions over a reaction time of hours (Endo, 2002). The DMAP ($C_7H_{10}N_2$) molecules attaching the colloidal gold have an appreciable dipole moment and a molecular diameter of about 10 Å.

2.1. Homogeneous mineralization

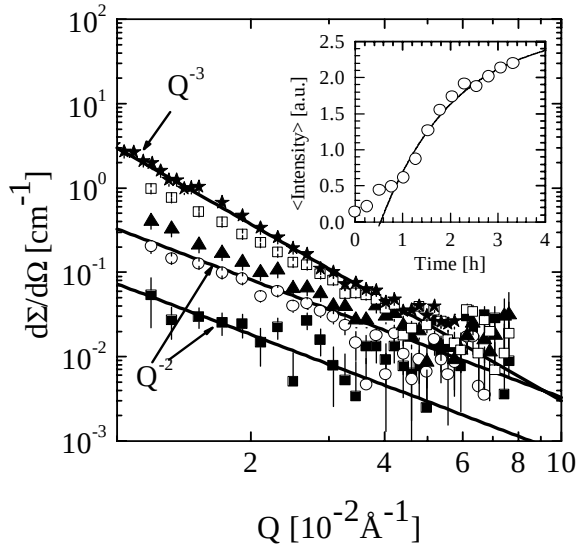

Figure 1

Time resolved scattering patterns from a homogeneous mineralization of $CaCO_3$ in H_2O at 303 K. A Q^{-2} shape of the scattering patterns was found from the beginning (■) and after 30 min (○) of mineralization. After 1 h (▲) a transition to a Q^{-3} shape is observed indicating the formation of porous 3D-particles after 1.5 (□) and 3.3 h (★). The measurement time was always 15 min and the given times represent the start of a measurement. The inset shows the intensity averaged over the given *Q* range versus time.

Scattering patterns from homogeneously mineralized $CaCO_3$ in water at 303 K (30°C) are presented in Fig.1. The macroscopic cross-section is depicted versus the modulus Q of the scattering vector in double (Note: double is log (log x)) logarithmic scales. The value of Q is determined according to

$$Q = 4\pi \sin(\theta/2)/\lambda \qquad (2)$$

from the neutron wave length λ and the scattering angle θ. The mineral nucleates into thin plates with a thickness less than 30 Å as concluded from the Q^{-2} power law behavior of the scattering patterns. After about 1 h (curve with symbol: ▲) a transition from a Q^{-2} to a Q^{-3} is observed indicating the growth regime of porous three-dimensional (3D) particles. The inset shows the intensity averaged over the given Q range versus time. The nucleation starts right from the beginning when the mineralization was started and leads to a stronger increase after 1 h when the growth process of the 3D-particles has started.

2.2. **Mineralization on DMAP templates**

Fig. 2 shows the scattering patterns of a mineralization process at 303 K (30°C) in the presence of 15 mg/cm^3 DMAP molecules. The first curve (circles) refers to the solution of DMAP, while the second refers to the sample in which the mineralization process has been active for 6 h. The DMAP molecules in water precipitate into a bimodal size distribution of large compact aggregates according to the Porod behavior at low Q and of smaller particles of roughly 20 Å. The solid lines represent a fit of the following scattering law

$$\frac{d\Sigma}{d\Omega}(Q) = P_1 Q^{-4} + \left\{ I_0 \exp(-u^2/3) + P_2 \left[\left(\mathrm{erf}\left(u/\sqrt{6}\right) \right)^3 / Q \right]^4 \right\} \qquad (3)$$

describing the scattering from particles larger than of the order of 1000 Å due to the smallest Q of 0.002Å^{-1} by the Porod constant P_1 and from smaller ones by the second term. The parameters have the following meaning: $u = R_g Q$ with the radius of gyration R_g; $I_0 = C V^2$ representing the forward scattering of the smaller particles and being proportional to the square of the particle volume V and the constant $C = N_p \Delta\rho^2$, determined by the particle number density N_p, and the difference of the coherent scattering length density $\Delta\rho$ of the particle and water; the Porod constant $P_2 = 2\pi CS$ with S the particle surface area. The scattering law for the smaller particles in (3) was formulated by Beaucage (1995) for particles of spherical shape from the approximate forms of the Guinier and Porod laws being valid for Q smaller and larger than the inverse radius of gyration $1/R_g$, respectively (R.-J. Roe, 2000 on p.167 and p.178). The radius R of spheres is either evaluated from the radius of gyration according to $R = \sqrt{(5/3)}\, R_g$, or from the particle volume and surface area as derived from I_0 and P_2, respectively. A possible non-spherical shape of the particles can be derived from these parameters. Such non-spherical particles were indeed observed in the present study indicating plate-shaped particles. But such a detailed analysis will not be discussed here.

The SANS data in Fig.2 show that the DMAP molecules are not dissolved as discrete molecules; calculations show that under such circumstances their scattering would be too weak to be detected because of their small size and low volume fraction.

After a mineralization period of 6 h a strong increase of intensity is found; according to the bimodal structure of the template molecules large and small compact minerals have been formed during the mineralization process, the smaller ones of about 300 Å radius.

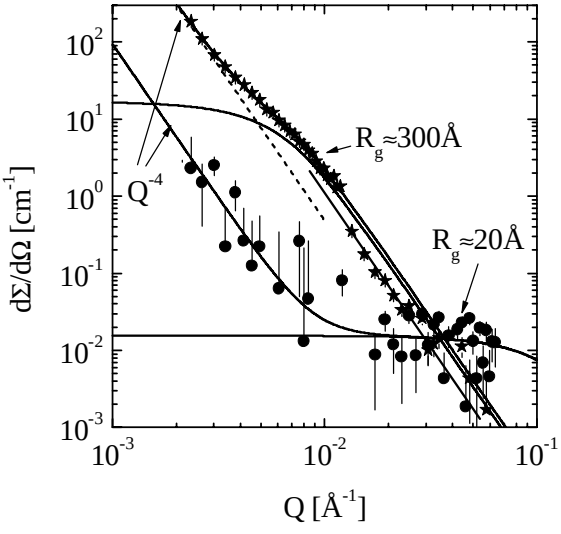

Figure 2

Small-angle scattering before (●) and after 6 h of mineralization (★) in the presence of 15 mg/cm^3 DMAP molecules at 303 K (30°C).

2.3. **Mineralization on DMAP plus gold templates**

Fig.3 shows the process of mineralization in the presence of 49 mg/cm^3 gold plus DMAP molecules at 303 K (30°C). Again we find indications of large aggregates mainly consisting of DMAP molecules as followed from contrast variation measurements (Schwahn *et al.*, 2003) and smaller particles of 40 Å identified as colloidal gold attached with DMAP. Smaller DMAP aggregates are

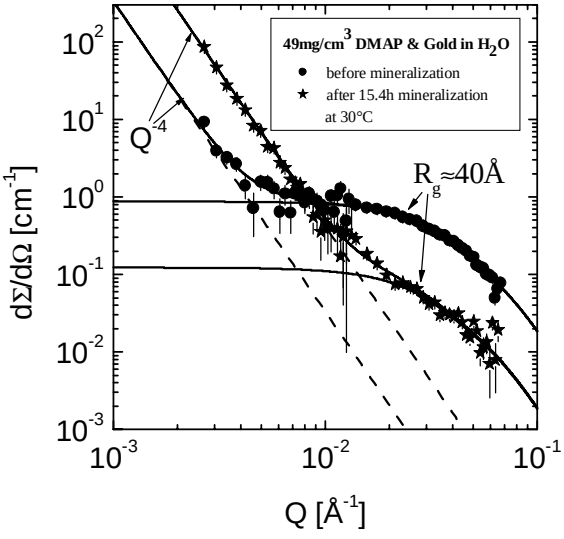

Figure 3

Before and after 15 hrs of mineralization at 30°C in the presence of 49mg/cm^3 DMAP and colloidal gold.

not visible as the scattering from the gold particles is dominating. After slightly more than 15 h mineralization time an order of magnitude increase of intensity is measured indicating an increased amount of larger particles. Surprisingly, the size of smaller particles does not increase due to mineralization but decreases in number density. It seems that under these experimental conditions the mineralization process leads to an aggregation of the smaller gold particles into the already existing larger DMAP aggregates.

3. Discussion and Conclusions

In Figs. 4,5 the time evolution of characteristic parameters of the large and small particles evaluated from the SANS data are presented. In Fig.4 the time evolution of the radius of gyration and Porod constant of the smaller and larger particles are shown for two samples; one sample only with DMAP as discussed in Fig.2, the other with a low concentration of 5 mg/cm^3 gold plus DMAP. These two samples show at least qualitatively the same mineralization behavior. The smaller particles do not change for the first 2 h and then increase to a value of R_g of about 350 Å after 6 h. Their growth behavior is slightly different but their incubation time is the same. The same behavior is also found for the Porod constant of the larger particles. No incubation time is visible. The growth velocity is relatively low during the first hour, but then speeds up appreciably and starts to saturate after about 4 h.

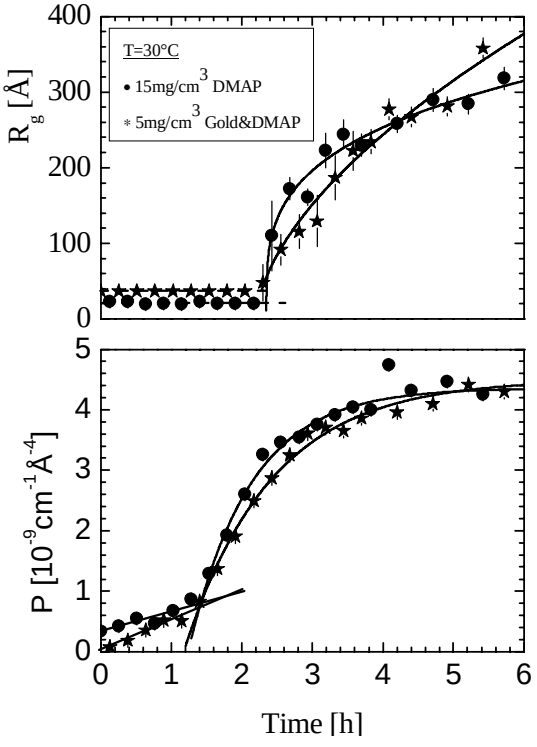

Figure 4

Top: Evolution of the radius of gyration of the "smaller" particles by mineralization.
Bottom: Same process for the larger particles as characterized by the Porod constant being proportional to the total surface area.

A quite different result is found in Fig.5 for the sample with higher DMAP plus gold concentration of 49 mg/cm^3 which has already been discussed in context with Fig.3. The time evolution of the Porod constant of the larger particles in the lower figure is very similar to that in Fig.4. A smaller growth velocity during the first hour, then a strong increase, and saturation and slight decrease after six hours. In the discussion of the results presented in Fig.3 we have mentioned that the size of the smaller particles stays constant within a standard deviation of ±2.3 Å and with a mean R_g=37.2 Å. Actually, at the beginning of mineralization we observe a slightly larger size of 40 Å which then continuously decreases during the first 1.5 h. The upper panel of Fig.5 shows the evolution of the product of the particle number density and the square of the difference of the coherent scattering length density $\Delta\rho^2$ of particle and solvent. As the coherent scattering length density of gold and $CaCO_3$ is about the same with $\rho\approx4.5\times10^{10}$cm^{-2} one evaluates a $\Delta\rho^2=2.6\times10^{21}$cm^{-4} considering the corresponding value for water $\rho=-0.56\times10^{10}$cm^{-2}. The number density stays relatively constant during the first 4 h and then strongly decreases reducing the number after eight hours by more than a factor of 5. After eight hours only a slight decrease is observed. Comparing number density and Porod constant in the upper and lower panels of Fig.5, a correlation between both processes is clearly visible. Along with the strong decrease of the

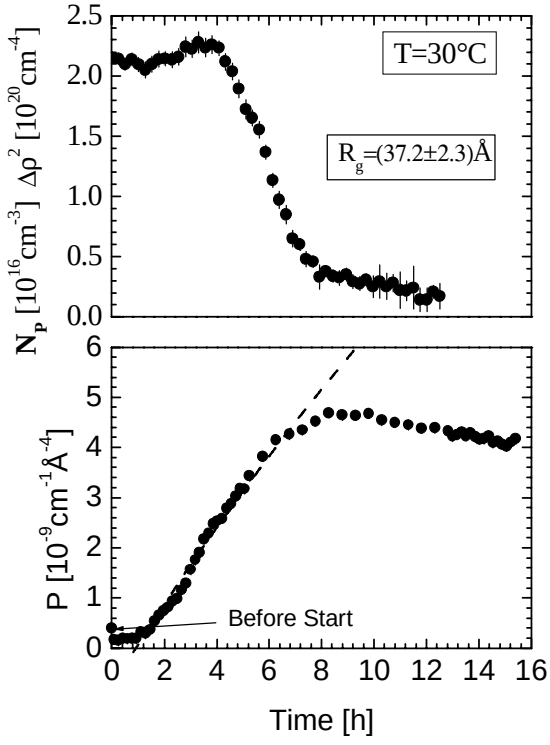

Figure 5

Top: Particle number density times the scattering contrast versus time in a solution of 49 mg/cm^3 gold plus DMAP at 30°C (same as in Fig. 3). During this process a constant size of the smaller particles of R_g=37Å is observed. Between 4 and 8 hours a strong decrease of the number density is observed.
Bottom: Porod constant of the larger particles versus time. Saturation and decrease of P due to coarsening occur after 8h when the strong decrease of the smaller particles stops. This result is an indication that the smaller particles aggregate into the larger ones.

amount of smaller particles the Porod constant is increasing. Saturation of the Porod constant is achieved when about 80% of the smaller particles are used up after eight hours mineralization time and only a small further decrease with time is observed. This clearly indicates that the smaller particles aggregate into the larger ones and thus drive their coarsening.

The observation of two mineralization processes for the smaller particles as a function of the template concentration and temperature is a rather surprising result and not yet understood. To give a better survey we plotted in Fig. 6 a diagram whose axes represent the conditions of mineralization, namely temperature and DMAP plus gold concentration. The positions of the symbols represent the experimental conditions while the symbols •,*, and ▲ themselves represent the characteristics of observations, namely, coarsening by the increase of R_g , aggregation as discussed in Fig.5, and the sample without any gold as discussed in Fig. 4, respectively. The dashed line roughly separates the both regions of coarsening and aggregation.

A possible interpretation of the different coarsening mechanisms might be that (1) the colloidal gold always aggregate into the larger ones while (2) the observed coarsening of the smaller particles at lower temperature and concentration occurs at the smaller DMAP clusters of 20 Å as measured in Fig. 2. These smaller DMAP aggregates might always be present but not visible in the presence of colloidal gold. One could imagine that these smaller DMAP

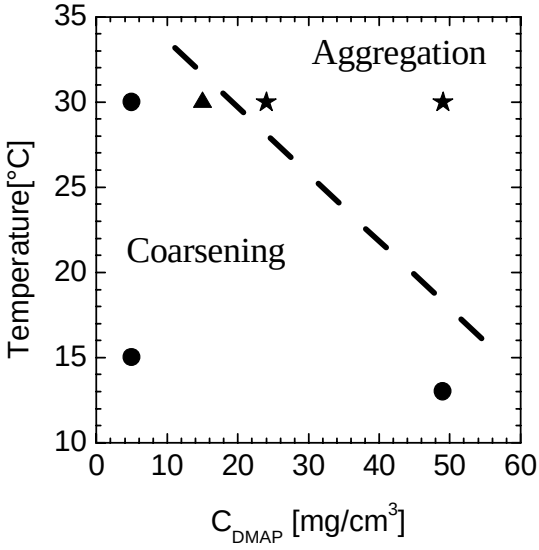

Figure 6

Diagram showing the external conditions for the two coarsening mechanisms of the "smaller" particles. Separated by the dashed line a coarsening process is observed at low temperature and DMAP concentration. Aggregation as shown in Fig. 5 is found at larger temperatures and DMAP concentration.

aggregates become unstable above a given temperature and concentration and decompose into discrete molecules which may not be active with respect to the mineralization of $CaCO_3$. The experimental background of this speculation are the results in Fig.4 showing for the same temperature at 303 K (30°C) similar time evolution of the smaller and larger particles.

4. Summary and Outlook

In this article we presented first results on the process on $CaCO_3$ mineralization in an aqueous solution in the presence of a template structure build up by DMAP molecules and of 40 Å radius colloidal gold covered with DMAP, thereby offering a large surface. The process of mineralization was performed in a 0.1 M aqueous calcium dichloride solution with the gas diffusion technique using an ammonium carbonate precursor (see equation (1)). In this way, the mineralization was sufficiently slow for the neutron experiments. While $CaCO_3$ in water nucleates into thin (<30Å) plates and subsequently grows into large porous objects the mineralization in the presence of DMAP molecule templates always leads to 3D compact $CaCO_3$ particles.

The original goal was of course to have a single template structure determined by the surface of the colloidal gold. However, the reality turned out to be more complex showing at least three different template structures of large (>1000 Å) and small (≈20 Å) mainly DMAP aggregates and the colloidal gold covered with DMAP. Such a template structure of course leads to a formation of minerals whose original nucleation center is not always easy to survey.

In near future we will focus on studies of the DMAP phase behavior and try to better analyze the concentrations within the different phases by applying the contrast variation technique. In addition, we will fill the diagram of external conditions in Fig.6 with more data points and try to better understand the two different mechanisms of mineralization.

This work was performed within the "Schwerpunktprogramm" of "Principles of Biomineralization" funded by the German Science Foundation.

References

Beaucage, G. (1995). *J. Appl. Cryst.* **28**, 717-728.
Gittins. D.I. & Caruso, F. (2001). *Angew. Chemie* **113**, 3089-3092
Endo, H., Cölfen, H. & Schwahn, D. (2003). *J. Appl. Cryst.* **36**, 568-572.
Endo, H.(2002). (private communication)
Mann, S: (2000) *Angew. Chem.*, **112**, 3532-3548
Roe, R.-J. (2000). *Methods of X-Ray and Neutron Scattering in Polymer Science*. Oxford: Oxford University Press.
Schwahn, D., Balz, M. & Tremel, W. (2003). In preparation.